

UniLVSeg: Unified Left Ventricular Segmentation in Echocardiograms through Weakly and Self-Supervised Training

Fadillah Maani, Asim Ukaye, Nada Saadi, Numan Saeed, and Mohammad Yaqub

Abstract— Echocardiography has become an indispensable clinical imaging modality for general heart health assessment. From calculating biomarkers such as ejection fraction to the probability of a patient’s heart failure, accurate segmentation of the heart and its structures allows doctors to plan and execute treatments with greater precision and accuracy. However, achieving accurate and robust left ventricle segmentation is time-consuming and challenging due to different reasons. Hence, clinicians often rely on segmenting the left ventricular (LV) in two specific echocardiogram frames to make a diagnosis. This limited coverage in manual LV segmentation makes it challenging to develop automatic LV segmentation with high temporal consistency since the resulting datasets are annotated sparsely. This work introduces a novel approach for consistent left ventricular (LV) segmentation from sparsely annotated echocardiogram videos. We achieve this through (1) self-supervised learning (SSL) using temporal masking followed by (2) weakly supervised training. We investigate two different segmentation approaches: 3D segmentation and a novel 2D superimage (SI). We demonstrate how our proposed method outperforms the state-of-the-art solutions by achieving a 93.32% (95%CI 93.21-93.43%) dice score on a large-scale dataset (EchoNet-Dynamic) while being more efficient. To show the effectiveness of our approach, we provide extensive ablation studies, including pre-training settings and various deep learning backbones. Additionally, we discuss how our proposed methodology achieves high data utility by incorporating unlabeled frames in the training process. To help support the AI in medicine community, the complete solution with the source code will be made publicly available upon acceptance.

Index Terms— Left Ventricle Segmentation, Sparse Video Segmentation, 3D Segmentation, Super Image, Self-supervision, Temporal Masking.

I. INTRODUCTION

ECOCARDIOGRAMS are a crucial modality in cardiovascular imaging due to their safety, availability, and high temporal resolution [2]. In clinical practice, echocardiogram information is used to diagnose heart conditions and understand the preoperative risks in patients with cardiovascular diseases [3]. Through heart-beat sequences in echocardiogram videos, clinicians measure ejection fraction value to determine

Fadillah Maani, Asim Ukaye, Nada Saadi, Numan Saeed, and Mohammad Yaqub are with the Department of Computer Vision, Mohammed Bin Zayed University of Artificial Intelligence (MBZUAI), Abu Dhabi, UAE (e-mail: fadillah.maani@mbzuai.ac.ae).

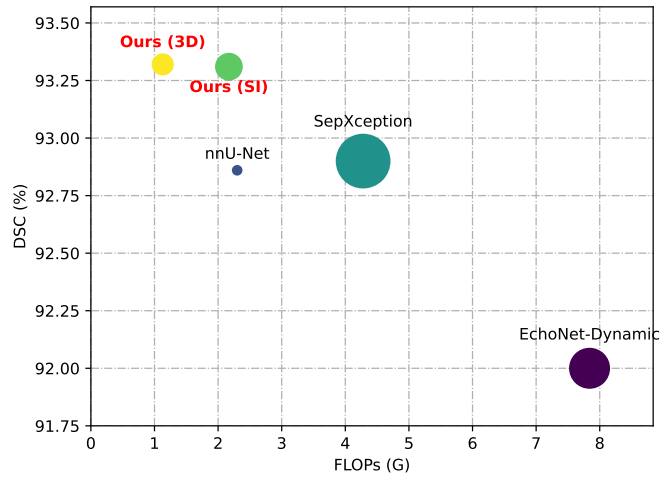


Fig. 1: A comparison with other state-of-the-art solutions. Our methods achieve higher DSC on the EchoNet-Dynamic test set while being more efficient. The bubble size represents the number of parameters.

whether the heart can supply adequate oxygenated blood to the entire body. The ejection fraction reflects the percentage of blood the heart can pump out of the left ventricular (LV), which is calculated as $(EDV - ESV)/EDV$ using the LV volume in the end-diastole (ED) phase end-systole (ES) phase. ED refers to the phase where the heart is maximally filled with blood just before contraction, while the ES phase happens immediately after the contraction where the volume of heart chambers is in its minimum stage. By accurately segmenting the heart structures, especially the ED and ES frames, clinicians can assess the extent and location of the disease, determine the appropriate treatment approach, and monitor the patient’s response to therapy [4].

The typical manual workflow of segmenting LV is as follows: 1) a sonographer acquires an echocardiogram video using an ultrasound device and records the patient’s heartbeat, 2) finds ED and ES by locating candidate frames indicated by the recorded heartbeat signal and then verifies them visually with the recorded echocardiogram video, 3) draws some key points to represent LV region as shown in Figure 2. That manual LV segmentation workflow is typically time-consuming and prone to intra- and inter-observer variability. The inherent

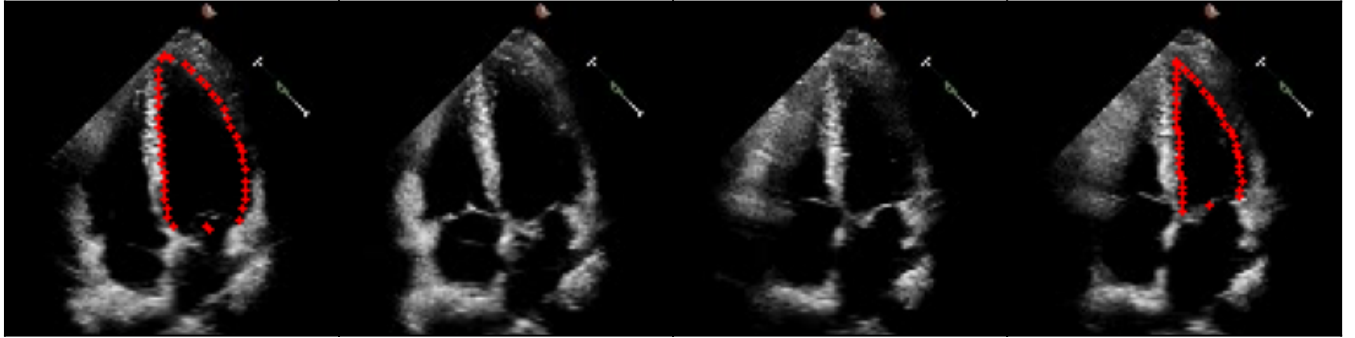


Fig. 2: A sequence of an echocardiogram video [1]. The number of frames varies, yet only two are labeled, i.e. the end-diastole (left-most) and the end-systole (right-most) frame. Annotators draw key points to represent the left ventricular (LV) region. Then, LV segmentation labels are inferred from the given key points.

speckle noise in echocardiograms makes LV segmentation more challenging, as LV boundaries are sometimes unclear. Hence, sonographers need to consider the temporal context to eliminate the ambiguity caused by unclear heart structures in echocardiograms and perfectly segment LV to achieve accurate results. It can even add more burden for sonographers since they must go back-and-forth between echocardiogram frames to analyze the ambiguous boundaries properly. Automatic LV segmentation can help sonographers in solving this arduous task more efficiently.

A wide range of work on performing medical image segmentation using a supervised deep-learning approach is presented [5], [6]. Earlier segmentation approaches on echocardiograms propose a frame-by-frame (2D) image segmentation solution [1], [7]–[10]. The image-based approaches however, do not capitalize on the periodicity and temporal consistency of the echocardiograms, which may lead to incoherence in the segmentation results from one frame to the next. In the worst-case scenario, the incoherence can lead to the ED and ES phase detection failure in the fully automatic ejection fraction prediction pipeline [1]. This has motivated a recent body of video-based echocardiogram segmentation approaches.

Li et al. [11] use a Conv-LSTM to ensure spatiotemporal consistency between consecutive frames. Ahn et al. [12] use a multi-frame attention network to perform 3D segmentation. Wu et al. [13] demonstrated the effectiveness of semi-supervision using mean-teacher networks and spatiotemporal fusion on segmentation. Recently, Wei et al. [14] propose a two-stage training to enforce temporal consistency on a 3D U-Net by leveraging an echocardiogram ED & ES sequence constraint. Painchaud et al. [15] improve the average segmentation performance by enforcing temporal smoothness as a post-processing step on video segmentation outputs.

These video-based approaches show high temporal consistency and state-of-the-art performance. However, they pose certain limitations. Recurrent units in [11] incur a high computational cost. Multi-frame attention in [12] similarly has computational cost correlated to the number of frames and they are limited to using five frames. Wu et al. [13] limit the temporal context to three frames to obtain optimum performance-compute trade-off. Wei et al. [14] leverages a

constraint in their training pipeline where the segmented area changes monotonically as the first input frame is ED and the last frame is ES in the same (*one*) heartbeat cycle, thus limiting the usage of vastly unannotated frames in other cycles.

Moreover, publicly available echocardiogram datasets such as [1] and [16] have only two annotated frames per video, i.e. end-diastole (ED) and end-systole (ES) frames. In the case of the EchoNet-Dynamic dataset [1], this utilizes less than 1.2 % of the available frames when training in a 2D supervised setting. Self-supervised learning (SSL) alleviates this problem. Saeed et al. [17] use contrastive pre-training to provide self-supervision on echocardiograms. Recently, He et al. [18] show that masked autoencoders (MAE) for self-supervised pre-training enables accelerated training and improves accuracy on natural image-based tasks. Feichtenhofer et al. [19] and Tong et al. [20] extend this idea to spatiotemporal masking and show promising results on action recognition.

On the other hand, image-based networks are computationally cheaper and retain an advantage in being effectively pre-trained on a large corpus of annotated image datasets. Annotated video datasets are, in comparison, more scarce. Fan et al. [21] introduced the idea of super images by flattening videos into image grids and successfully performed video-based tasks such as action recognition using image classifiers. Sobirov et al. [22] employ this approach on medical images for atrial and head and neck cancer segmentation problems.

The aforementioned works perform LV segmentation from echocardiogram videos **either by** 1) analyzing frames independently with simple 2D deep learning models **or** 2) performing 2D+time analysis and developing models using complex training schemes. In our proposed method, while achieving state-of-the-art performance, we aim to mimic clinical assessment where doctors assess multiple frames concurrently in a simplified approach. We introduce a novel self-supervised pre-training approach and a loss calculation method for video-based echocardiogram segmentation, specifically designed to handle sparsely annotated frames in the downstream task. Our *key contributions* are:

- We propose a *self-supervised temporal masking* approach that leverages vastly unannotated echocardiogram frames to provide a better network initialization for the down-

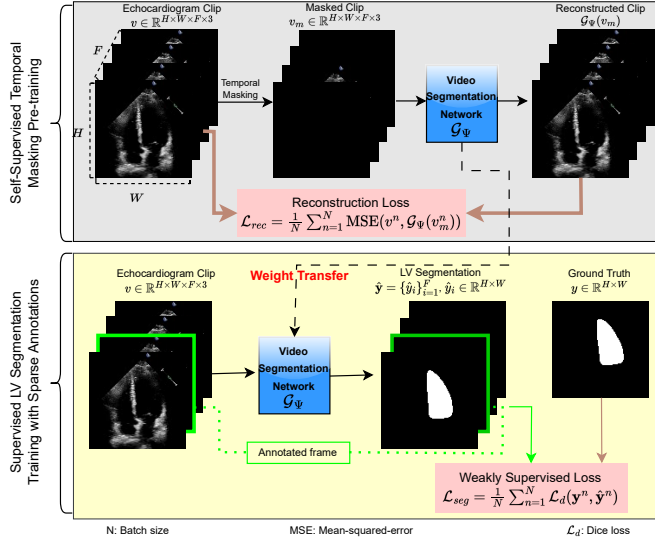


Fig. 3: An illustration of our approach. A video segmentation network is developed to segment LV on every input echocardiogram frame. The network is pre-trained using a self-supervised temporal masking method, which is then fine-tuned on the LV segmentation task with sparse annotations.

stream LV segmentation task by learning the periodic nature of echocardiograms.

- We propose a loss calculation mechanism that allows a video-based segmentation network to learn LV segmentation from *sparsely annotated* echocardiogram videos without any heartbeat cycle constraint.
- We show the compatibility of our approach with the 2D super image and 3D segmentation network with various encoder backbones.
- We demonstrate how our proposed approach outperforms the state-of-the-art in LV segmentation on Echonet-Dynamic in terms of performance and efficiency through extensive ablation studies.

II. METHODOLOGY

Our proposed method is demonstrated in Figure 3. The network utilizes unannotated frames for a pre-training stage and learns from annotated frames in a weakly-supervised manner. The performance of the proposed method was evaluated with 3D segmentation and 2D super image (SI) segmentation [21] approach, as depicted in Figure 4. The details are described below.

A. Self-Supervised Temporal Masking.

In the EchoNet-Dynamic [1] dataset, most of the frames are unannotated, thus the ability to perform supervised training is limited. To benefit from the vast amount of unlabeled frames, we implement a self-supervised temporal masking algorithm to pre-train our model. As depicted in Figure 3, a clip of an echocardiogram video is retrieved, and a portion of the frames is masked. The model is then pre-trained to reconstruct the masked clip. Through this process, the model

learns valuable latent information from the periodic nature of echocardiograms, e.g. the embedded temporal pattern or cardiac rhythm, that benefit the downstream LV segmentation task.

More formally, suppose V is an echocardiogram video with $H \times W$ frame size. From V , we sample a clip $v \in \mathbb{R}^{H \times W \times F \times 3}$ consisting of F number of consecutive frames with a stride or sampling period of T . Then, we provide a masked clip $v_m \in \mathbb{R}^{H \times W \times F \times 3}$ by randomly choosing F_m number of frames ($F_m < F$) from v and adjusting their pixel values to 0. A video network \mathcal{G}_Ψ with a set of parameters Ψ is then pre-trained to reconstruct v from v_m . The network \mathcal{G}_Ψ is optimized by minimizing the following objective:

$$\mathcal{L}_{rec} = \frac{1}{N} \sum_{n=1}^N \text{MSE}(v^n, \mathcal{G}_\Psi(v_m^n)) \quad (1)$$

where N is the batch size.

B. LV Segmentation with Sparse Annotations

The sparsely-annotated echocardiogram videos make the LV segmentation challenging as training a video segmentation model on EchoNet-Dynamic is not trivial. To tackle the issue, inspired by [23], we propose a training strategy to develop a video segmentation network specifically for LV. As illustrated in Figure 3, the network takes in F number of frames and segments the LV on each frame. Then, the loss is calculated and backpropagated only based on the prediction of frames having a segmentation label.

More formally, let \mathcal{G}_Ψ be the pre-trained video segmentation network which takes in an input echocardiogram clip $v \in \mathbb{R}^{H \times W \times F \times C}$ and predicts LV segmentation $\hat{y} = \{\hat{y}_1, \hat{y}_2, \dots, \hat{y}_F\}$, $\hat{y}_i \in \mathbb{R}^{H \times W}$, where F , C , and $H \times W$ are the number of frames, the number of channels which is 3, and the frame size, respectively. Also, let $y = \{y_1, y_2, \dots, y_F\}$, $y_i \in \mathbb{R}^{H \times W}$ denote the sparse segmentation label of the input clip where most y_i are empty. Thus, we construct y for every sample by using the following rule:

$$y_i = \begin{cases} y_i & \text{if } i\text{-th frame is labeled} \\ \emptyset & \text{otherwise} \end{cases} \quad (2)$$

Thus, the total dice loss \mathcal{L}_d for every sample n can be formulated as:

$$\begin{aligned} \mathcal{L}_d(y^n, \hat{y}^n) &= \sum_{i=1}^F \ell_d(y_i^n, \hat{y}_i^n) \\ &= \underbrace{\sum_{j \in \mathcal{F}_l^n} \ell_d(y_j^n, \hat{y}_j^n)}_{\text{labeled (annotated) frames}} + \underbrace{\sum_{k \in \{1, \dots, F\} \setminus \mathcal{F}_l^n} \ell_d(y_k^n, \hat{y}_k^n)}_{\text{unlabeled frames}} \end{aligned} \quad (3)$$

where ℓ_d is the *frame-wise* dice loss, and \mathcal{F}_l^n is the set of indices of labeled frames for the n -th sample. The gradient of

\mathcal{L}_d w.r.t. a parameter $\psi \in \Psi$ is given by:

$$\begin{aligned} \frac{\partial \mathcal{L}_d}{\partial \psi}(\mathbf{y}^n, \hat{\mathbf{y}}^n) &= \sum_{j \in \mathcal{F}_i^n} \frac{\partial \ell_d}{\partial \psi}(y_j^n, \hat{y}_j^n) \\ &+ \sum_{k \in \{1, \dots, F\} \setminus \mathcal{F}_i^n} \frac{\partial \ell_d}{\partial \psi}(y_k^n, \hat{y}_k^n) \end{aligned} \quad (4)$$

where $\frac{\partial \ell_d}{\partial \psi}(y_k^n, \hat{y}_k^n)$ can be simply set to zero because the k -th frame is unlabeled, preventing the unlabeled frames from contributing to the gradients. Since (1) $\hat{y}_j \in \mathcal{G}_\Psi(v)$, and (2) \mathcal{G}_Ψ typically consists of shared-weights operators (e.g. convolution and attention), then

$$\begin{aligned} \frac{\partial \ell_d}{\partial \psi}(y_j^n, \hat{y}_j^n) \in \mathbb{R} &\implies \sum_{j \in \mathcal{F}_i^n} \frac{\partial \ell_d}{\partial \psi}(y_j^n, \hat{y}_j^n) \in \mathbb{R} \\ &\implies \frac{\partial \mathcal{L}_d}{\partial \psi}(\mathbf{y}^n, \hat{\mathbf{y}}^n) \in \mathbb{R} \end{aligned} \quad (5)$$

for all parameters ψ in Ψ . Thus, although a clip v is partially labeled and gradients do not come from unlabeled frames, *this framework can facilitate training for all \mathcal{G}_Ψ parameters*. Ultimately, the total segmentation loss is given by:

$$\mathcal{L}_{seg} = \frac{1}{N} \sum_{n=1}^N \mathcal{L}_d(\mathbf{y}^n, \hat{\mathbf{y}}^n) \quad (6)$$

During training, a clip is randomly extracted around an annotated frame from every video with the specified number of frames F and sampling period T , resulting in more variations and acting as a regularizer. In other words, there is only a segmentation mask for one frame on every clip. To reduce randomness during the evaluation step, a clip is extracted from each video where an annotated frame is at the center of the clip.

C. Video Segmentation

We aim to develop a video segmentation network \mathcal{G}_Ψ capable of segmenting LV from an echocardiogram clip $v \in \mathbb{R}^{H \times W \times F \times C}$. We consider two segmentation approaches as visualized in Fig. 4, i.e. the 3D segmentation approach and the 2D super image (SI) approach. The 3D approach considers an echocardiogram clip as a 3D volume, while the SI approach addresses the video segmentation problem in a 2D fashion [22]. We describe the details of both approaches below.

1) *3D Segmentation Approach*: Echocardiogram videos consist of stacked 2D images. Considering the time axis as the 3rd dimension allows 3D models to segment the LV on an echocardiogram clip. Thus, the 3D U-Net [23] is utilized as the architecture. As depicted in Fig. 5, we use a CNN with residual units [24] as the encoder, which has 5 stages where the stage outputs are passed to the decoder. A residual unit comprises two Conv2D layers, two instance norm layers, two PReLU activation functions, and a skip connection.

2) *2D Super Image Approach*: An echocardiogram clip v is rearranged into a single big image $x \in \mathbb{R}^{\hat{H} \times \hat{W} \times C}$, where \hat{H} and \hat{W} are the height and width of the SI respectively. Since the SI works best with a grid layout [21], we set the

echocardiogram SI size to be $H\sqrt{F} \times W\sqrt{F}$. Hence, existing techniques for 2D image analysis can be well utilized to help solve the problem, e.g. state-of-the-art architectures, self-supervised methods, and strong pre-trained models.

The 2D U-Net [5] is used as the main architecture with the UniFormer-S [25] as the encoder. We select the UniFormer-S since 1) it leverages the strong properties of convolution and attention, and 2) it is the recent state-of-the-art on EchoNet-Dynamic ejection fraction estimation [26]. In short, the network consists of 4 stages, where the first two stages utilize convolution operators to extract features, and the rest implement multi-head self-attention (MHSA) to learn global contexts. The inductive biases of convolution layers allow the model to learn efficiently and the MHSA has a large receptive field that is favorable for SI [21].

III. EXPERIMENTAL SETUP

Experiments were performed on EchoNet-Dynamic [1], a large-scale echocardiography dataset, using an NVIDIA RTX 6000 GPU with CUDA 11.7 and PyTorch 1.12.

A. Dataset

We conducted our experiments on the EchoNet-Dynamic dataset [1]. EchoNet-Dynamic is the largest publicly available 2D+Time echocardiograms of the apical four-chambers (A4C) view of the human heart. The dataset comprises approximately 10,030 heart echocardiogram videos with a fixed frame size of 112×112 . Video length varies from 28 to 1002 frames, yet only two are annotated (ED & ES frames). A sample echocardiogram sequence is given in Figure 2.

To ensure a fair comparison with reported state-of-the-art methods, we adhered strictly to the organizer's provided split, consisting of 7460 training videos, 1288 validation videos, and 1276 test videos.

B. Implementation Details

We pre-trained our video segmentation models for 100 epochs with self-supervision. Each echocardiogram video was randomly sampled on every epoch with a specified number of frames (F) and a stride or sampling period (T) to give more variations. We utilized the AdamW optimizer and set the learning rate to 3e-4 learning rate and weight decay to 1e-5. A set of augmentations was applied to enrich the variation during training, consisting of color jitter, CLAHE, random rotation, padding to 124×124 frame size, and random cropping to 112×112 . Then, the model is fine-tuned for the LV segmentation task with sparse annotations in a weakly-supervised manner for 70 epochs. Every video was sampled twice on every epoch to accommodate the annotated ED and ES frames. Hyper-parameters were set experimentally.

IV. RESULTS

A. Comparison with the state-of-the-art

Our method outperforms recent state-of-the-art approaches ([1], [6], [10]) on the EchoNet test set, as shown in Table I and Figure 1. We compare our method with the approach

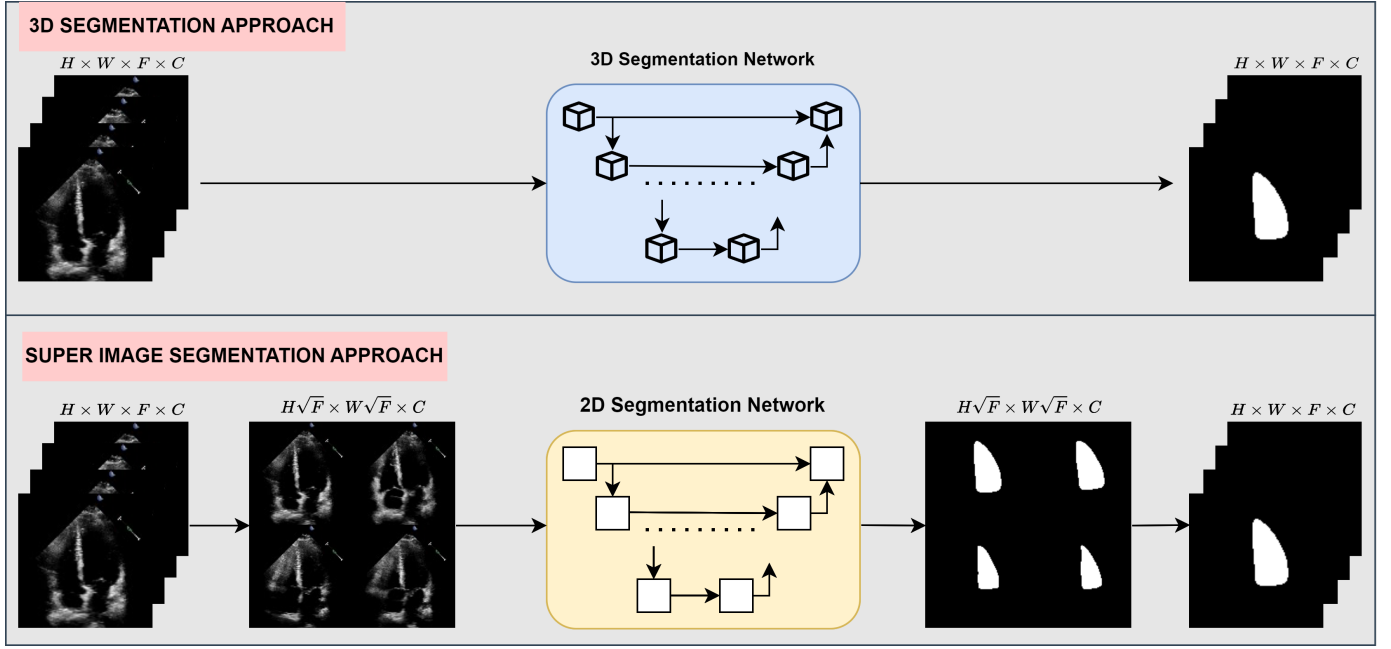


Fig. 4: The 3D vs. 2D super image segmentation approach. The first approach utilizes a 3D segmentation network, while the second rearranges the echocardiogram clip as a super image and then utilizes a 2D network.

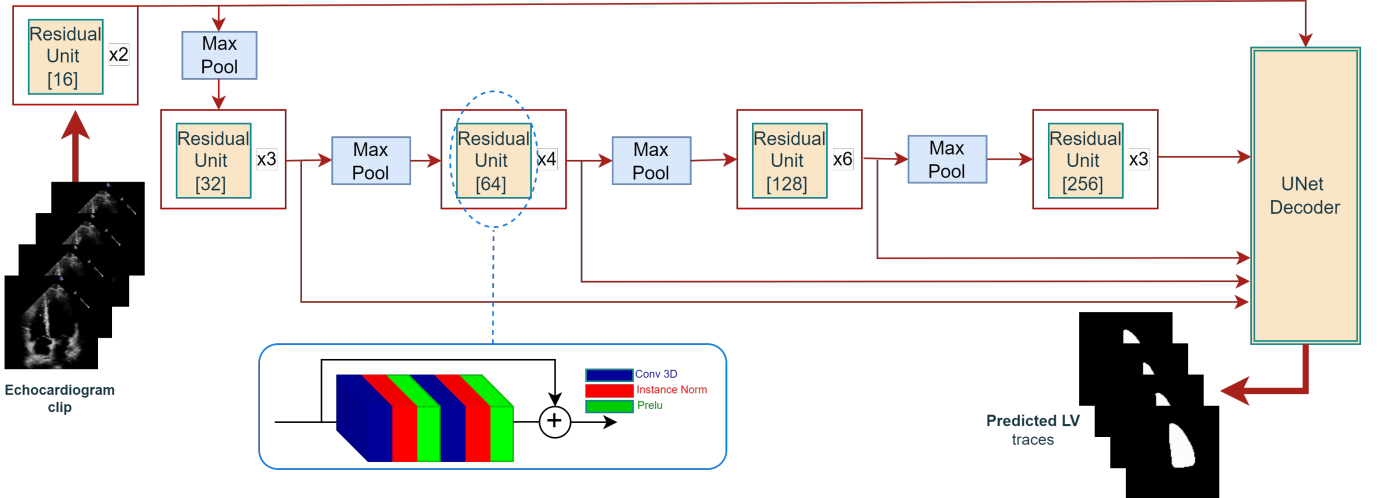


Fig. 5: The 3D U-Net architecture. A residual unit [24] consists of convolutional layers, instance norm layers, PReLU, and a skip connection. Residual Unit [C] denotes a residual unit with C number of feature channels.

proposed by the EchoNet dataset publisher [1], the famous nnU-Net [6], which can perform better than specially designed echocardiography networks as mentioned in [27], and the method achieving the highest dice similarity coefficient (DSC) on the test set [10] (to the best of our knowledge). Our 3D U-Net results in 93.32% overall DSC, and the SI approach shows on-par performance. Confidence interval (CI) analysis further shows no overlap between the 95% CI of our methods with other state-of-the-art solutions, indicating that our improvements hold statistical significance over those methods with a *p-value* of less than 0.05. Our 3D U-Net was trained with 32 frames sampled consecutively, while the SI was trained with 16 frames sampled at every 5th frame. This experiment shows that a video segmentation network trained

in a weakly-supervised manner is capable of segmenting the LV with a 3.8x lower computational cost compared to [10].

B. Ablation studies

1) *Number of Frames and Sampling Period*: The number of frames F and the sampling period T play important roles [13], [26]. Large F allows a network to retrieve rich temporal information while increasing T reduces redundancy between frames. We studied the combination of (F, T) to find the optimum pair as provided in Table II. The (16, 5) combination results in the highest DSC of 93.21% for SI while (32, 1) gives the best performance for 3D approach, resulting in 93.31% DSC. Additionally, all (F, T) pairs result in a better performance compared to [10].

TABLE I: Dice similarity coefficient (DSC) on EchoNet-Dynamic test set. Our approach shows state-of-the-art performance with fewer FLOPs and relatively fewer parameters. fvcore was utilized to count the FLOPs. Note that we report FLOPs on a per-frame basis (*).

Method	DSC (95%CI)				FLOPs (G)	#Params (M)
	Overall		ES	ED		
EchoNet-Dynamic [1]	92.00 (91.87-92.13)	90.68 (90.55-90.86)	92.78 (92.61-92.94)	7.84	39.64	
nnU-Net [6]	92.86 (92.74-92.98)	91.63 (91.43-91.83)	93.62 (93.48-93.76)	2.30	7.37	
SepXception [10]	92.90 -	91.73 (91.54-91.92)	93.64 (93.50-93.78)	4.28	55.83	
Ours (SI)	93.31 (93.19-93.43)	92.26 (92.08-92.44)	93.95 (93.81-94.09)	(*) 2.17	24.83	
Ours (3D)	93.32 (93.21-93.43)	92.29 (92.11-92.47)	93.95 (93.81-94.09)	(*) 1.13	18.83	

TABLE II: An ablation study on the number of frames Net was trained from scratch. All reported values are overall DSC (%) scores.

Approach	<i>F</i>	Sampling Period			
		1	2	3	5
2D Super Image (UniFormer-S)	4	93.06	93.12	93.17	93.09
	9	93.11	93.14	93.15	93.13
	16	93.17	93.13	93.18	93.21
	25	93.16	93.11	93.20	93.12
3D U-Net	16	93.23	93.25	93.11	93.04
	32	93.31	93.14	93.06	92.90

TABLE IV: An ablation study on various encoder backbones. Our approach is robust to the selection of backbone complexity. The SI backbones were pre-trained on the ImageNet dataset, while the 3D U-Net-S was trained from scratch.

Approach (# Frames, Period)	Backbone	% DSC (Overall)	Params (M)	FLOPs (G)	
				Single pass	One frame
Super Image (SI) (16, 5)	MobileNetV3	93.16	6.69	12.46	0.78
	ResNet-18	93.23	14.33	21.75	1.36
	ViT-B/16	92.98	89.10	120.20	7.51
3D (32, 1)	3D U-Net-S	93.27	11.26	27.34	0.85

2) *SSL Temporal Masking*: We conducted an ablation study (Table III) to find the optimum value of the masking ratio and obtain the best results for 60 % masking. We find that SSL pre-training helps maintain better temporal consistency and improve robustness (Fig. 6).

3) *Different backbones*: An ablation study was performed on different encoders of the segmentation architecture to see how well our approach adapts to model complexity. We implemented ResNet-18 [28], MobileNet-V3 [29], and ViT-B/16 [30] as the encoder of the SI approach. We also tested with a smaller version of 3D U-Net (Fig. 5), which consists of two residual units on every stage (3D U-Net-S). As provided in Table IV, the experiment shows that the performance is robust to encoder backbones.

V. DISCUSSIONS

Table I shows that while being more efficient, our video segmentation networks outperform the highest reported DSC on the EchoNet-Dynamic test set. Our networks aggregate both spatial and temporal information by analyzing multiple

echocardiogram frames at a single pass. The networks predict an LV segmentation trace for every input frame at once, thus eliminating the redundancy in analyzing the same frames multiple times as in [27] and [13]. In addition, our training pipeline is simple yet effective, easy to implement, and scalable, as it does not require pseudo labels [14], [31] or temporal regularization [15]. Compared to [14], [31], our proposed approach does not depend on a specific heart stage, thus eliminating the burden of locating the ED and ES frame when creating training data. This also allows us to easily exploit non-ED and -ES frames for supervision if their corresponding segmentation labels are available. Table II highlights the robustness of our approach to the sampling hyperparameters. This allows for a broader design space to meet hardware limitations such as memory and compute power (FLOPs) while still achieving a satisfactory segmentation performance.

We observed that randomly masking a significant portion (60%) of an echocardiogram clip during SSL pre-training results in the best performance. The masking SSL improves the overall DSC of the SI approach from 93.19% to 93.31%,

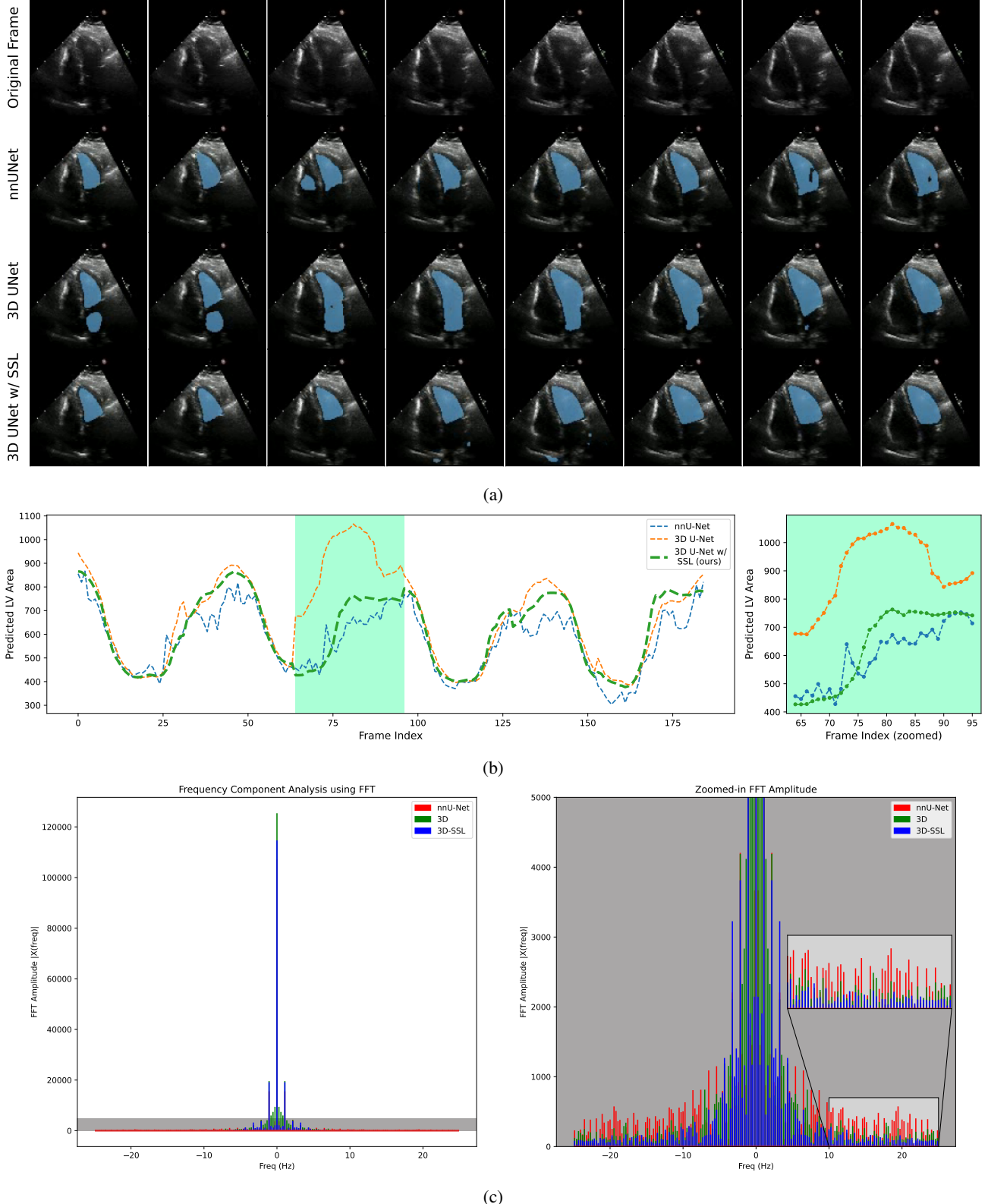


Fig. 6: Qualitative results for the performance of nnU-Net (2D) [6], 3D U-Net, and 3D U-Net with self-supervision without any post-processing trick against a challenging case where the Mitral valve is unclear. (a) We observe that the 3D U-Net with self-supervised temporal masking pre-training is more resilient to noise and missing artifacts in the input frames. (b) The predicted LV segmentation area is smoother and more consistent for the 3D-SSL approach compared to others. A zoomed version of the plot for is shown on the right. (c) Frequency analysis using FFT on the predicted LV areas shows a lower magnitude of high-frequency components (i.e. lower noise) in the 3D-SSL approach as compared to others.

as reported in Table III. Further, as shown in Fig. 6, we observe that self-supervision with temporal masking enables the network to maintain better temporal consistency across predictions in a given echocardiogram clip. Fig. 6a demonstrates that a video segmentation model pre-trained with self-supervised temporal masking is more resilient to noise and missing artifacts. The pre-training stage also alleviates the over-segmentation and temporal inconsistency issues that are commonly encountered in echocardiography caused by unclear (or, even worse, invisible) boundaries. Also, the SSL pre-trained model achieves a smoother LV segmentation area prediction with significantly less rapid fluctuations (see Fig. 6b), indicating better temporal consistency. We further investigate the phenomenon in the frequency domain by applying the Fast Fourier Transform (FFT) to the predicted signals (LV area) as depicted in Fig. 6c. We observe that SSL pre-training results in a lower magnitude of the high-frequency components, which are typically the result of noise and rapid fluctuation. Based on these observations, we hypothesize that the pre-training stage helps the 3D U-Net model to better learn the semantic features that are useful for estimating human heart structures in the A4C view, resulting in a more robust prediction. These findings indicate that pre-training with self-supervision remarkably benefits the downstream LV segmentation task. Hence, self-supervised learning with vast echocardiogram videos can be a promising solution to provide strong pre-trained models that can generalize well in downstream echocardiography-related clinical tasks.

We have shown that both the SI and 3D methods trained using sparse annotations are capable of accurately segmenting the left ventricle in echocardiogram videos. The 3D U-Net performance is slightly better than the SI network with the UniFormer-S backbone. However, designing a backbone for 3D U-Net is not straightforward since it requires tedious hyperparameter tuning. On the other hand, there are plenty of optimized models that can be utilized as a backbone for the SI approach. For instance, MobileNetV3, with only 6.69 M of parameters, can give an on-par performance with 93.16% overall DSC, as can be seen in Table IV. The pre-trained models on ImageNet can also help generalize better if we only have a small data. Moreover, many self-supervised learning algorithms for 2D can also be employed to further improve performance.

VI. CONCLUSION

We propose a novel approach to tackle the LV segmentation task on echocardiogram videos. Our method outperforms other works on the EchoNet-Dynamic test set. The method utilizes a video segmentation network that efficiently combines both spatial and temporal information. The network is pre-trained on a reconstruction task and then trained with sparse annotations to predict LV. An extensive experiment was performed to show the superiority of the proposed approach both quantitatively and qualitatively. We expect that this work will motivate researchers to explore more about the video segmentation approach for LV instead of working on frame-by-frame prediction.

We limit our experiments in this work to self-supervision using temporal masking only. However, there remains scope to improve the self-supervision by identifying the optimum masking scheme between temporal, random spatiotemporal, space-wise, and block-wise masking. Further, we aim to validate the cross-dataset generalizability of our approach using other publicly available echocardiogram datasets.

REFERENCES

- [1] D. Ouyang, B. He, A. Ghorbani, N. Yuan, J. Ebinger, C. P. Langlotz, P. A. Heidenreich, R. A. Harrington, D. H. Liang, E. A. Ashley *et al.*, “Video-based ai for beat-to-beat assessment of cardiac function,” *Nature*, vol. 580, no. 7802, pp. 252–256, 2020.
- [2] S. J. Horgan and S. Uretsky, “Echocardiography in the context of other cardiac imaging modalities,” in *Essential Echocardiography: A Companion to Braunwald’s Heart Disease*. Elsevier, 2019, pp. 460–473.
- [3] M. K. Ford, W. S. Beattie, and D. N. Wijesundera, “Systematic review: prediction of perioperative cardiac complications and mortality by the revised cardiac risk index,” *Annals of internal medicine*, vol. 152, no. 1, pp. 26–35, 2010.
- [4] P. A. Heidenreich, J. G. Trogdon, O. A. Khavjou, J. Butler, K. Dracup, M. D. Ezekowitz, E. A. Finkelstein, Y. Hong, S. C. Johnston, A. Khera *et al.*, “Forecasting the future of cardiovascular disease in the united states: a policy statement from the american heart association,” *Circulation*, vol. 123, no. 8, pp. 933–944, 2011.
- [5] O. Ronneberger, P. Fischer, and T. Brox, “U-net: Convolutional networks for biomedical image segmentation,” in *MICCAI 2015*, N. Navab, J. Hornegger, W. M. Wells, and A. F. Frangi, Eds. Cham: Springer International Publishing, 2015, pp. 234–241.
- [6] F. Isensee, P. F. Jaeger, S. A. A. Kohl, J. Petersen, and K. H. Maier-Hein, “nnU-Net: a self-configuring method for deep learning-based biomedical image segmentation,” *Nature Methods*, vol. 18, no. 2, pp. 203–211, Feb. 2021.
- [7] E. Smistad, A. Østvik, B. O. Haugen, and L. Løvstakken, “2d left ventricle segmentation using deep learning,” in *2017 IEEE International Ultrasonics Symposium (IUS)*, 2017, pp. 1–4.
- [8] Y. Hu, L. Guo, B. Lei, M. Mao, Z. Jin, A. Elazab, B. Xia, and T. Wang, “Fully automatic pediatric echocardiography segmentation using deep convolutional networks based on bisenet,” in *2019 41st Annual International Conference of the IEEE Engineering in Medicine and Biology Society (EMBC)*, 2019, pp. 6561–6564.
- [9] S. Leclerc, E. Smistad, T. Grenier, C. Lartizien, A. Østvik, F. Cervenansky, F. Espinosa, T. Espeland, E. A. Rye Berg, P.-M. Jodoin, L. Løvstakken, and O. Bernard, “Ru-net: A refining segmentation network for 2d echocardiography,” in *2019 IEEE International Ultrasonics Symposium (IUS)*, 2019, pp. 1160–1163.
- [10] E. Chen, Z. Cai, and J.-h. Lai, “Weakly supervised semantic segmentation of echocardiography videos via multi-level features selection,” in *Pattern Recognition and Computer Vision*, S. Yu, Z. Zhang, P. C. Yuen, J. Han, T. Tan, Y. Guo, J. Lai, and J. Zhang, Eds. Cham: Springer Nature Switzerland, 2022, pp. 388–400.
- [11] M. Li, W. Zhang, G. Yang, C. Wang, H. Zhang, H. Liu, W. Zheng, and S. Li, “Recurrent aggregation learning for multi-view echocardiographic sequences segmentation,” in *MICCAI 2019: 22nd International Conference, Proceedings, Part II 22*. Springer, 2019, pp. 678–686.
- [12] S. S. Ahn, K. Ta, S. Thorn, J. Langdon, A. J. Sinusas, and J. S. Duncan, “Multi-frame attention network for left ventricle segmentation in 3d echocardiography,” in *MICCAI 2021: Proceedings, Part I 24*. Springer, 2021, pp. 348–357.
- [13] H. Wu, J. Liu, F. Xiao, Z. Wen, L. Cheng, and J. Qin, “Semi-supervised segmentation of echocardiography videos via noise-resilient spatiotemporal semantic calibration and fusion,” *Medical Image Analysis*, vol. 78, p. 102397, 2022.
- [14] H. Wei, J. Ma, Y. Zhou, W. Xue, and D. Ni, “Co-learning of appearance and shape for precise ejection fraction estimation from echocardiographic sequences,” *Medical Image Analysis*, vol. 84, p. 102686, 2023. [Online]. Available: <https://www.sciencedirect.com/science/article/pii/S1361841522003140>
- [15] N. Painchaud, N. Duchateau, O. Bernard, and P.-M. Jodoin, “Echocardiography segmentation with enforced temporal consistency,” *IEEE Transactions on Medical Imaging*, vol. 41, no. 10, pp. 2867–2878, 2022.

[16] S. Leclerc, E. Smistad, J. Pedrosa, A. Østvik, F. Cervenansky, F. Espinosa, T. Espeland, E. A. R. Berg, P.-M. Jodoin, T. Grenier *et al.*, “Deep learning for segmentation using an open large-scale dataset in 2d echocardiography,” *IEEE transactions on medical imaging*, vol. 38, no. 9, pp. 2198–2210, 2019.

[17] M. Saeed, R. Muhtaseb, and M. Yaqub, “Contrastive pretraining for echocardiography segmentation with limited data,” in *Medical Image Understanding and Analysis: 26th Annual Conference, MIUA 2022, Proceedings*. Springer, 2022, pp. 680–691.

[18] K. He, X. Chen, S. Xie, Y. Li, P. Dollár, and R. Girshick, “Masked autoencoders are scalable vision learners,” *arXiv:2111.06377*, 2021.

[19] C. Feichtenhofer, H. Fan, Y. Li, and K. He, “Masked autoencoders as spatiotemporal learners,” *arXiv:2205.09113*, 2022.

[20] Z. Tong, Y. Song, J. Wang, and L. Wang, “VideoMAE: Masked autoencoders are data-efficient learners for self-supervised video pre-training,” in *Advances in Neural Information Processing Systems*, 2022.

[21] Q. Fan, C.-F. Chen, and R. Panda, “Can an image classifier suffice for action recognition?” in *International Conference on Learning Representations*, 2022.

[22] I. Sobirov, N. Saeed, and M. Yaqub, “Segmentation with super images: A new 2d perspective on 3d medical image analysis,” *arXiv preprint arXiv:2205.02847*, 2022.

[23] Ö. Çiçek, A. Abdulkadir, S. S. Lienkamp, T. Brox, and O. Ronneberger, “3d u-net: learning dense volumetric segmentation from sparse annotation,” in *MICCAI 2016: Proceedings, Part II 19*. Springer, 2016, pp. 424–432.

[24] E. Kerfoot, J. Clough, I. Oksuz, J. Lee, A. P. King, and J. A. Schnabel, “Left-ventricle quantification using residual u-net,” in *Statistical Atlases and Computational Models of the Heart. Atrial Segmentation and LV Quantification Challenges*, M. Pop, M. Sermesant, J. Zhao, S. Li, K. McLeod, A. Young, K. Rhode, and T. Mansi, Eds. Cham: Springer International Publishing, 2019, pp. 371–380.

[25] K. Li, Y. Wang, J. Zhang, P. Gao, G. Song, Y. Liu, H. Li, and Y. Qiao, “Uniformer: Unifying convolution and self-attention for visual recognition,” *CoRR*, vol. abs/2201.09450, 2022. [Online]. Available: <https://arxiv.org/abs/2201.09450>

[26] R. Muhtaseb and M. Yaqub, “Echocotr: Estimation of the left ventricular ejection fraction from spatiotemporal echocardiography,” in *MICCAI 2022*, L. Wang, Q. Dou, P. T. Fletcher, S. Speidel, and S. Li, Eds. Cham: Springer Nature Switzerland, 2022, pp. 370–379.

[27] S. Thomas, A. Gilbert, and G. Ben-Yosef, “Light-weight spatio-temporal graphs for segmentation and ejection fraction prediction in cardiac ultrasound,” in *MICCAI 2022: 25th International Conference, Proceedings, Part IV*. Springer, 2022, pp. 380–390.

[28] K. He, X. Zhang, S. Ren, and J. Sun, “Deep residual learning for image recognition,” in *2016 IEEE Conference on Computer Vision and Pattern Recognition, CVPR 2016*. IEEE Computer Society, 2016, pp. 770–778.

[29] A. Howard, R. Pang, H. Adam, Q. V. Le, M. Sandler, B. Chen, W. Wang, L. Chen, M. Tan, G. Chu, V. Vasudevan, and Y. Zhu, “Searching for mobilenetv3,” in *2019 IEEE/CVF International Conference on Computer Vision, ICCV 2019*. IEEE, 2019, pp. 1314–1324.

[30] A. Dosovitskiy, L. Beyer, A. Kolesnikov, D. Weissenborn, X. Zhai, T. Unterthiner, M. Dehghani, M. Minderer, G. Heigold, S. Gelly, J. Uszkoreit, and N. Houlsby, “An image is worth 16x16 words: Transformers for image recognition at scale,” in *9th International Conference on Learning Representations, ICLR 2021*, 2021.

[31] H. Wei, H. Cao, Y. Cao, Y. Zhou, W. Xue, D. Ni, and S. Li, “Temporal-consistent segmentation of echocardiography with co-learning from appearance and shape,” in *MICCAI 2020: 23rd International Conference, Proceedings, Part II 23*. Springer, 2020, pp. 623–632.